analytical chemistry

Article

Cite This: Anal. Chem. 2019, 91, 6652−6660

pubs.acs.org/ac

Highly Sensitive Lab on a Chip (LOC) Immunoassay for Early Diagnosis of Respiratory Disease Caused by Respirable Crystalline Silica (RCS)

V. Thiyagarajan Upaassana,[†] Sthitodhi Ghosh,[†] Atreyee Chakraborty,[†] M. Eileen Birch,[‡] Pius Joseph,[§] Jungyoup Han,[∥] Bon Ki Ku,*[,‡] and Chong H. Ahn*[,†]

[†]Microsystems and BioMEMS Laboratory, Department of Electrical Engineering and Computer Science, University of Cincinnati, Cincinnati, Ohio 45221, United States

[‡]Centers for Disease Control and Prevention (CDC), National Institute for Occupational Safety and Health (NIOSH), Division of Applied Research and Technology, 1090 Tusculum Avenue, Cincinnati, Ohio 45226, United States

[§]Centers for Disease Control and Prevention (CDC), National Institute for Occupational Safety and Health (NIOSH), Health Effects Laboratory Division, 1095 Willowdale Road, Morgantown, West Virginia 26505, United States

[∥]Mico BioMed USA Inc., 10999 Reed Hartman Highway, STE 309C, Cincinnati, Ohio 45242, United States

ABSTRACT: Respirable crystalline silica (RCS) produced in mining and construction industries can cause life-threatening diseases such as silicosis, lung cancer, and chronic obstructive pulmonary disease (COPD). These diseases could be more effectively treated and prevented if RCS-related biomarkers were identified and measured at an early stage of disease progression, which makes development of a point of care test (POCT) platform extremely desirable for early diagnosis. In this work, a new, highly sensitive lab on a chip (LOC) immunoassay has been designed, developed, and characterized for tumor necrosis factor α (TNF-α), a protein biomarker that causes lung inflammation due to RCS exposure. The designed LOC device is composed of four reservoirs for sample, enzyme conjugated detection antibody, wash buffer, and chemiluminescence substrate in liquid form, along with three spiral reaction chambers for test, positive control, and negative control. All reservoirs and spiral microchannels were connected in series and designed to perform sequential delivery of immunoassay reagents with minimal user intervention. The developed LOC measured TNF-α concentrations as low as 16 pg/mL in plasma from RCS-exposed rats and also had a limit of detection (LOD) of 0.5 pg/mL in spiked artificial serum. In addition, the analysis time was drastically reduced to about 30 min, as opposed to hours in conventional methods. Successful implementation of a highly sensitive, chemiluminescence-based immunoassay on a preloaded LOC with proper quality control, as reported in this work, can pave the way toward developing a new rapid POCT platform for in-field clinical diagnosis.

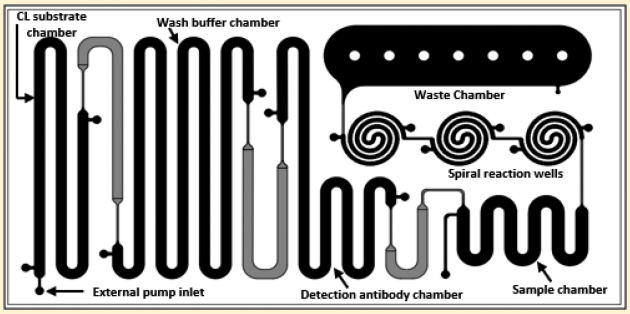

INTRODUCTION

Approximately two million U.S. workers were reported to be routinely exposed to airborne respirable crystalline silica (RCS).[1] In particular, workers in the mining, hydraulic fracturing, and construction industries have significant health issues due to RCS exposure.[2,3] Inhalation of RCS, in the form of fractured sand produced by cutting, breaking, crushing, drilling, or grinding of coal, can cause silicosis, lung cancer, and/or chronic obstructive pulmonary disease (COPD). Recent National Institute for Occupational Safety and Health (NIOSH) field studies identified RCS levels in several work environments that exceeded safe levels of exposure by factors of 20 or more.[3−5] Approximately 600000 workers employed in the U.S. oil and gas extraction industry and 200000 U.S. workers in the mining and construction industries have the risk of being exposed to airborne RCS on a regular basis.[6−9] In early 2016, the U.S. Occupational Safety and Health Administration (OSHA) announced a new occupational exposure limit for RCS (50 $\mu g/m^3$, 8 h time-weighted average (TWA) in all industries).[7] Hence, exposure to RCS is considered as one of the major causes of significant occupational health problems in the United States.[1,8]

Early monitoring and detection (i.e., early-stage biomonitoring of RCS-exposed workers, before disease onset) of pulmonary responses to silica exposure such as lung inflammation and oxidative stress, as well as early identification of any silicosis initiation, are of great importance in disease prevention from the perspectives of occupational health surveillance and future epidemiological research. The clinical detection of silicosis is dependent on the detection of

Received: January 31, 2019
Accepted: April 23, 2019
Published: April 23, 2019

DOI: 10.1021/acs.analchem.9b00582
Anal. Chem. 2019, 91, 6652−6660

Scheme 1. Reliable, easy to Use, Field-Portable Biomonitoring Instrument for Point of Care (POC) Diagnostics: (a) Working Environment with Respirable Crystalline Silica (RCS); (b) On-Site Sampling and Lab on a Chip (LOC) Device; (c) POC Diagnostics with Handheld LOC Test Unit

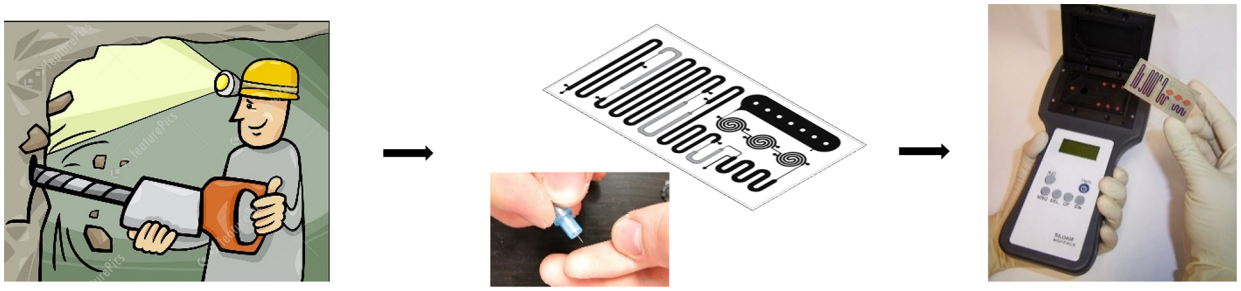

(a) (b) (c)

Scheme 2. Functional Concept of the Lab on a Chip with on-Chip Reservoirs in Operation Sequence To Perform Enzyme Immunoassay[18]

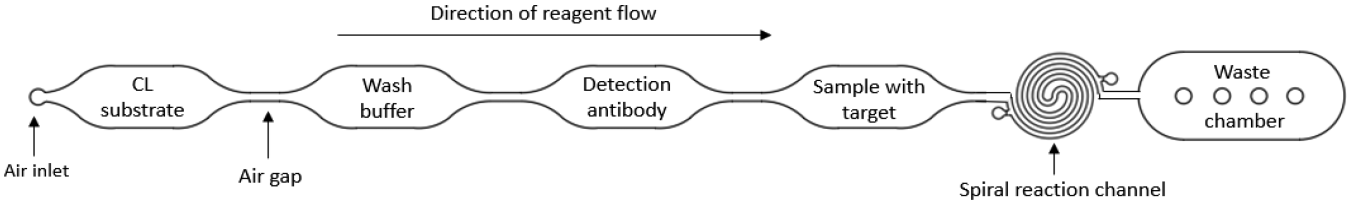

radiological abnormalities which are a late (10−15 years following exposure) and irreversible manifestation of the disease.[9] Once contracted, pulmonary diseases such as pneumoconiosis, silicosis, lung cancer, and COPD cannot be cured; therefore, it is crucial to prevent the development of these diseases by detecting early biological responses to exposure. Also, new data related to silica exposure and its health effects are of great interest to stakeholders for a better understanding of the exposure−response relationship. Although work environments are frequently monitored to determine air concentrations and occupational exposure to silica aerosol, relatively little biomonitoring or screening of exposed workers is performed due to lack of on-site biomonitoring devices. Currently available diagnostic procedures to identify lung inflammation and pulmonary diseases are based on chest radiography and conventional laboratory-based immunoassays, which are very bulky and take several days to provide clinically relevant data.[10−12] Additionally, they also require reagent preparation, trained personnel, and expensive instruments. Hence there is a significant need for cost-effective, reliable, easy to use, and field-portable biomonitoring instruments for rapid diagnostics, such as the point of care testing (POCT) platform illustrated in Scheme. 1. As shown in Scheme 1, an ideal POCT platform overcomes the disadvantages of conventional techniques by using only a drop of sample from workers which can be loaded onto a lab on a chip (LOC) and inserted into a field-portable analyzer for obtaining rapid quantitative results.

There has been a high demand for the development of POCT platforms for the early diagnosis of silicosis. For successful implementation, a POCT must offer robustness and portability, along with ultrahigh sensitivity and cost effectiveness.[13−18] Most of the existing immunoassay-based POCTs function using lateral flow assay methods, but the sensitivity of LOCs can be improved by implementing an LOC-based enzyme-linked immunosorbent assay (ELISA). Most studies on microfluidic immunoassays have involved multiple liquid-handling steps, which is a critical bottleneck toward their widespread use. Development of an automated, ELISA-based POCT platform would overcome drawbacks of the existing portable assays. Ideally, POCT should require minimal user intervention and be a sample to answer system, wherein the user only needs to add a sample to the LOC and can obtain clinically relevant data in a short time frame.[17] In this work, an LOC-based immunoassay has been designed, fabricated, and fully characterized for the detection of protein biomarkers of inflammation due to inhalation of silica aerosol. The polymer LOC has on-chip preloaded reservoirs that store all reagents required for the immunoassay, making it an ideal sample to answer system. The functional concept of the LOC is shown in Scheme 2. The device's serially connected reservoirs permit the sequential flow of reagents in the preloaded reservoirs, which is driven by air pressure at the device inlet, controlled by an external micropump. This design eliminates user intervention with external reagents and has a simplified system architecture which improves precision and can achieve quantitative and highly sensitive immunoassay results in the field. The LOC device, with its preloaded reagents, in combination with an externally controlled stop-flow incubation can perform a highly sensitive "sandwich" ELISA with CL-based detection.

EXPERIMENTAL SECTION

Design and Microfabrication of Immunoassay Lab-on-a-Chip. Biomarkers in blood such as tumor necrosis factor α (TNF-α), interleukin-6 (IL-6), IL-8, IL-1, neopterin, and Clara cell protein 16 (CC16) have been extensively explored as potential indicators of lung inflammation caused by exposure to silica aerosols.[19−24] In this work, an LOC-based ELISA for CL detection of TNF-α was developed and optimized. The LOC device was tested using plasma samples obtained from rats exposed to silica. A microfluidic LOC device for the

DOI: 10.1021/acs.analchem.9b00582
Anal. Chem. 2019, 91, 6652−6660

analysis of thyroid stimulating hormone (TSH) was developed and reported in our previous work.[18]

In this work, the previously reported device was redesigned and optimized to have three sensing spiral channels (test, positive control, and negative control), as shown in Figure 1.

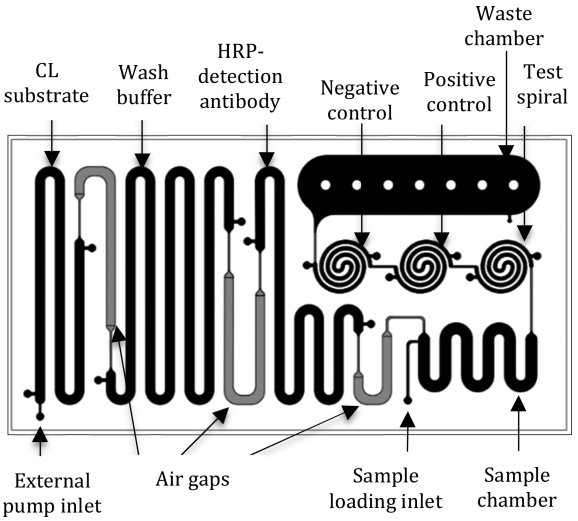

Figure 1. Schematic diagram of the lab on a chip illustrating on-chip reservoirs to store assay reagents. Air gaps isolate reagents and prevent mixing while in storage and during the assay. Spiral reaction chambers mimic the well structure present in conventional 96-well plates.

In addition, a sample loading chamber was added, so that plasma or serum sample can be prefilled before sequentially pushing it into the spiral reaction chambers. Clinically relevant biomarker levels are calculated from the optical signals detected from the test, positive control, and negative control spiral reaction chambers. All assay reagents are introduced sequentially by air-driven pumping from the air inlet of the LOC. As discussed, the CL-based immunoassay reagents are stored in the on-chip reservoirs designed to implement an ELISA using a single flow stream, where the liquid reagents are delivered to the spiral channels serially and sequentially. This eliminates the need for complex valves and pump systems to manipulate the microfluidic sequencing for the immunoassay. Air gaps and passive valves were inserted between the reagent chambers to ensure proper separation between the preloaded reagents. The air gap ensures reagent or sample separation during on-chip reagent storage and sequential delivery of reagents while the assay is performed. In the absence of air pressure from the external pump, the passive valves restrict the reagents inside their respective chambers and thus prevent unintentional reagent flow and mixing. Volumes of horseradish peroxidase (HRP) conjugated detection antibody, wash buffer, and CL substrate chambers were designed to accommodate enough reagent to perform the CL-based immunoassay in the spiral reaction chambers. In addition, a waste chamber was incorporated in the device to keep all used reagents and a potentially biohazardous sample inside the device, thus assuring safe and easy disposal of the LOC. The dimensions and volumes of the LOC are summarized in Table 1.

Microfabrication of Polymer Lab on a Chip. The microfabrication process used in this work consisted of master mold designing, aluminum master mold micromachining, and polymer chip replication by injection molding of cyclic olefin copolymer (COC).[25,26] For fabrication of a robust master mold with tall structures, a computer numerical control (CNC) micromilling process was chosen. The micromachining of the master mold was performed in three steps. First the LOC was designed using MasterCAM (CNC Software, USA) and then the milling tool paths for fabricating the master mold were created using the computer-aided manufacturing (CAM) programs (MasterCAM). Finally, the master mold was micromachined using a 5100-S CNC milling machine (Microlution, USA).

Table 1. Dimensions and Volume of Different Chambers in Designed LOC for Reagent and Sample Storage

reservoirs on LOC	width (mm)	length (mm)	height (mm)	volume (μL)
detection antibody chamber	1	72	0.35	25
wash buffer chamber	1	143	0.35	50
chemiluminescence substrate chamber	1	72	0.35	25
each of the spiral reaction chamber	0.35	45.7	0.25	4
sample loading chamber	1.2	44	0.35	18.5
air gap between each chamber	1	28.5	0.35	10

Aluminum alloy, Alloy 6061 (McMaster-Carr, USA), was used as the master mold material because it is flexibly machinable and can be used for several thousand replication cycles under optimized conditions. A thermoplastic polymer cyclic olefin copolymer (COC), 6013S (TOPAS Advanced Polymers), was used as the substrate material for the polymer LOCs. The COC material was chosen because of its high affinity toward protein adsorption, excellent resistance toward polar solvents, very high flow rates during injection molding, and high biological compatibility along with high optical clarity and low autofluorescence.[25,26] The short turnover time makes the process well suited for mass production. The COC LOCs were replicated by an injection molding process using a BOY 22A Procan CT apparatus (BOY, USA). The process cycle was automated, and the cycle time was optimized to 35 s per chip, thus ensuring a very low injection molding cost, which increased the throughput of the process. After replication, the injection-molded LOCs were drilled at specific inlet and outlet positions and then thermally bonded at 126 °C and 66 kPa to a blank COC chip, as summarized in Scheme 3. Thermal bonding was performed using a Hot Press P3H-15-CLX apparatus (Wabash MPI, USA). The micromachined master mold of the designed LOC and the replicated and bonded LOC with colored dyes are shown in Figure 2.

Assay Protocols and Validation. *Assay Kits and Reagents.* The sandwich ELISA of rat TNF-α was performed using the assay reagents from DuoSet ELISA DY510 (R&D Systems, USA). SuperSignal ELISA Pico Chemiluminescent (CL) Substrate, 37069 (Thermo Fisher Scientific), and Quanta Red Enhanced Chemifluorescent (CF) HRP Substrate, 15159 (Thermo Fisher Scientific), were used to perform the CL-based and CF-based assays, respectively. AffiniPure Goat Anti-Mouse IgG (H+L), 115-005-003 (Jackson Immunoresearch Laboratories, Inc.) was used as a positive control capture antibody. StartingBlock 37538 (Thermo Fisher Scientific) was used as a blocking buffer in the Optimiser microfluidic microplate and LOC assay. Serasub (CST Technologies, Inc.) was used for spiking different concentrations of rat TNF-α. A conventional 96-well plate reader, Synergy H1 (BioTek, USA), was used to read the conventional microplate, the Optimiser

DOI: 10.1021/acs.analchem.9b00582
Anal. Chem. 2019, 91, 6652−6660

Scheme 3. Schematic of COC LOC Fabrication Process: (a) Plasticization; (b) Clamping; (c) Molding; (d) LOC Ejection; (e) Thermal Bonding at 66 kPa and 126 °C; (f) Thermally Bonded COC LOC

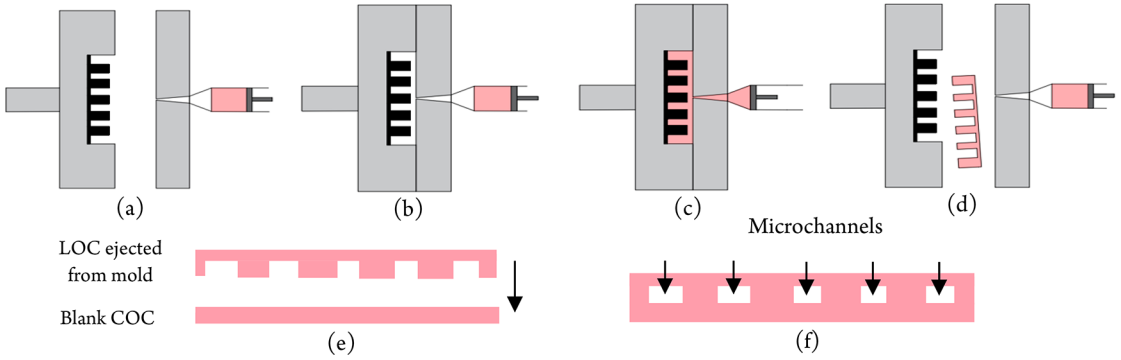

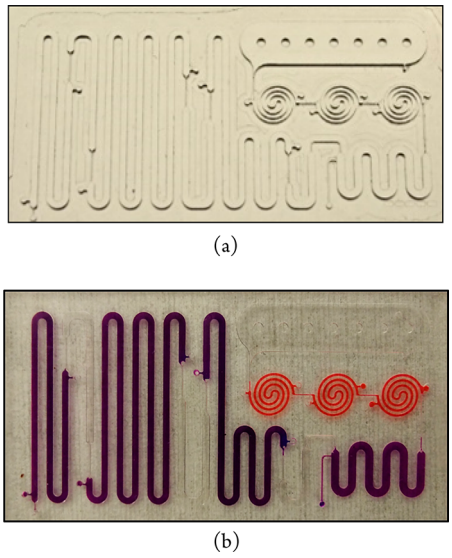

Figure 2. Fabrication of LOC: (a) micromachined aluminum master mold; (b) injection-molded and thermally bonded COC chip filled with colored dyes.

microfluidic microplate, and the LOC. A special LOC holder was made to fit the benchtop reader dimensions. All other assay reagents were from the DuoSet DY510 ELISA development kit (rat TNF-α) and an ELISA Ancillary Reagent Kit 2, DY008 (R&D Systems).

To develop and optimize an LOC-based immunoassay for CL detection of TNF-α, a commercially available sandwich ELISA kit for rat TNF-α (DuoSet ELISA DY510, R&D Systems, USA) was used as the standard reference. The assay was first performed using a conventional 96-well plate to verify the performance of the reagents. Because assay conditions and protocols for the microchannel-based LOC differ from those for a conventional 96-well plate, the assay parameters were optimized using the Optimiser microfluidic microplate (Mico BioMed USA Inc.), which has a spiral microfluidic channel in place of conventional well.[27] The spiral channels of the LOC developed in this work was designed to have the same dimensions as the spiral channel of the Optimizer microfluidic microplate. The unique microchannel geometry of the Optimiser microfluidic microplate[27] (Figure 3) requires a very small reagent volume (~4.5 μL) and favors rapid reaction kinetics, analogous to the designed LOC. Thus, the optimized assay conditions found from the Optimiser microfluidic microplate were applied to the microfluidic LOC, to perform

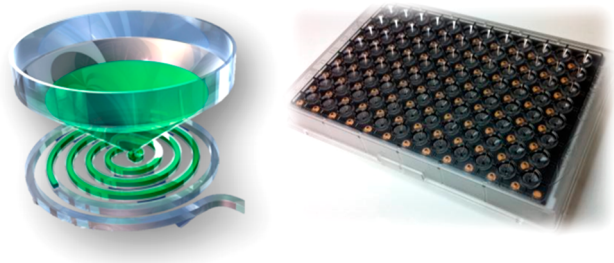

Figure 3. Optimiser microfluidic microplate with spiral microchannels (volume ~4.5 μL): (a, left) cell of spiral channel and (b, right) Optimiser microchannel plate.[29]

the CL-based TNF-α detection in artificial serum and rat plasma.

Reagent Validation by Conventional 96-Well Plate Assay. Assay optimization steps comprised of selecting the optimal capture (CAb) and detection (DAb) antibody concentrations and translating the well-established conventional 96-well plate assay to fit the LOC. The CL-based sandwich ELISA was performed on the developed LOC using the assay protocol described in Scheme 4. As a first step of optimization, the TNF-α sandwich ELISA was performed on a conventional 96-well plate following the vendor protocol. The standard curve (antigen concentration ranging from 62.5 pg/mL to 4.0 ng/mL, with 2-fold dilution in assay buffer) obtained from the optical output signal showed a typical linear trend similar to the vendor-provided reference graph[28] and validated the functionality of the assay reagents (Figure 4). Once the reagent functionality was confirmed with the conventional 96-well plate assay, Optimiser microfluidic microplates were used to determine the optimal antibody concentration for performing the same assay using microfluidic channels.

Antibody Optimization Using Optimiser Microfluidic Microplate. The unique microchannel geometry of the Optimiser microfluidic microplate offers several important advantages, vital for the development of a microchannel-based immunoassay. The rate of biological reaction in a microchannel largely depends on the rate of diffusion of the reagents, which in turn depends on the flow rate and the concentration of the reagents. Optimiser microfluidic microplates provide an environment similar to that of the designed microchannels on the LOC and act as excellent precursors to perform a CL assay on an LOC. Each of the 96 wells in an Optimiser microfluidic microplate has been replaced with a spiral microfluidic channel of volume 4.5 μL, as shown in Figure 3. Since CL has been

DOI: 10.1021/acs.analchem.9b00582
Anal. Chem. 2019, 91, 6652−6660

Scheme 4. Assay Protocol: (a) Immobilization of Capture Antibody and Blocking; (b) Binding of Target Biomarkers; (c) Selective Binding of Detection Antibodies Conjugated with HRP; (d) CL Substrate Addition Followed by Light Emission

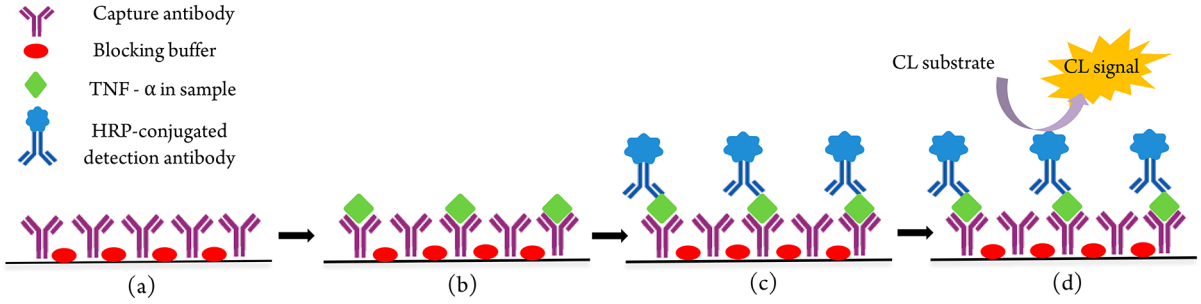

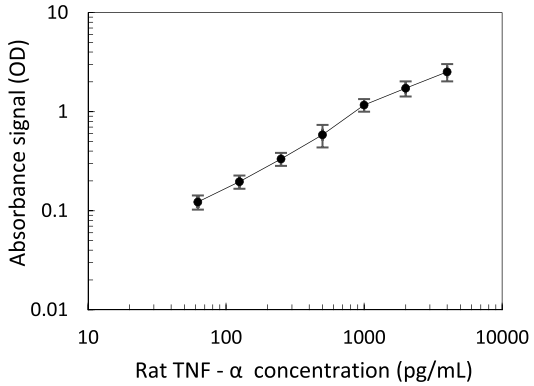

Figure 4. Standard curve obtained from a conventional 96-well plate assay for rat TNF-α detection which shows a typical linear trend similar to the vendor-provided reference graph.[28] Assay reagents were used from DuoSet ELISA DY510 (R&D Systems, USA), and each point represents the mean of three replicates.

reported to be a highly sensitive method of detection, the optimal antibody concentration obtained by performing a CF assay on the Optimiser microfluidic microplate can be reliably used for a CL-based assay on an LOC.[14,29]

To obtain the optimal antibody concentration, CF-based rat TNF-α detection was performed in an Optimiser microfluidic microplate using all the assay reagents at a fixed concentration except for the antibody to be optimized. The concentration of antibody to be optimized was varied over a wide range, and from the results of the assay, the antibody concentration value exhibiting the highest CF signal was determined to be the optimal concentration for all further assays (Assay Transfer Guide, Mico BioMed USA Inc., and Thermo-Scientific Pierce Assay Development Technical Handbook).[30,31]

All ELISAs in an Optimiser microfluidic microplate were performed on the basis of the following protocol: 5.0 μL of CAb was incubated for 20 min, followed by blocking for 10 min using 5.0 μL of StartingBlock buffer. A 5.0 μL sample containing TNF-α and HRP-conjugated DAb was incubated consecutively for 20 min, followed by a plate wash using 30.0 μL of phosphate buffer solution (pH 7.2−7.4). Then, 10 μL of QuantaRed Enhanced Chemifluorescent (CF) HRP Substrate was added and the plate was read after 15 min. A 2.0 ng/mL concentration of rat TNF-α antigen (assay buffer) was used for all optimization assays described in this section. To arrive at an appropriate value of the optimal CAb concentration, the DAb concentration was fixed at a high value of 1.6 μg/mL, while the CAb concentration was varied over a wide range, from 4.0 to 128.0 μg/mL.

As shown in Figure 5a, the highest CF signal corresponded to a CAb concentration of 16.0 μg/mL and gradually decreased with a further increase in the CAb concentration due to the "hook effect".[32] To confirm these results, optimization experiments were repeated using the LOC platform (with CL detection), and the results agreed with those obtained with the Optimiser microfluidic microplate. Thus, the optimized CAb concentration was fixed at 16.0 μg/mL.

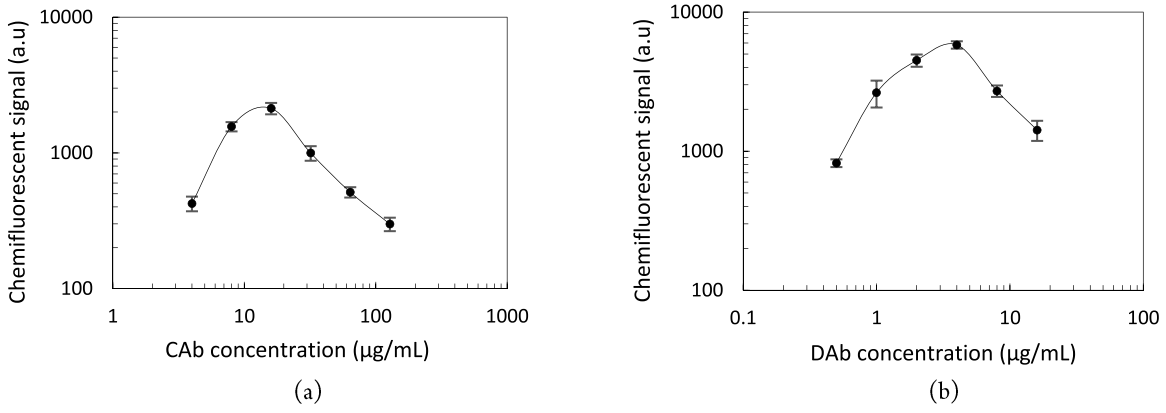

Figure 5. Antibody optimization curve obtained from an Optimiser microfluidic microplate. (a) CF signal variation with increase in capture antibody (CAb) for detection of TNF-α at a fixed DAb concentration of 1.6 μg/mL. Each point represents the mean of three replicates. (b) CF signal variation with increase in detection antibody (DAb) for detection of TNF-α at a fixed CAb concentration of 16.0 μg/mL. Each point represents the mean of three replicates.

DOI: 10.1021/acs.analchem.9b00582
Anal. Chem. 2019, 91, 6652−6660

For optimization of the detection antibody, the CAb concentration was fixed at the optimized value, 16.0 μg/mL, and the DAb concentration was varied from 0.5 to 32.0 μg/mL. The highest CF signal corresponded to a DAb concentration of 4.0 μg/mL and again gradually decreased (hook effect) with a further increase in the DAb concentration, as shown in Figure 5b. It can be noted from Figure 5 that CF signals obtained in DAb optimization experiments are higher than those obtained in CAb optimization experiments. The higher CF signal obtained in the DAb optimization experiment is due to the use of an optimized CAb concentration (16.0 μg/mL) in performing those assays, whereas in the case of the CAb optimization experiment, the DAb concentration was fixed at a nonoptimized concentration of 1.6 μg/mL. Similar to rat TNF-α antibody optimization, positive control capture antibody was also optimized to be 5.0 μg/mL for the LOC assay.

Two key features of the LOC microchannels are high surface to volume ratio and low sample volume. Increasing the antibody concentrations increases the probability and extent of antigen binding, resulting in a higher signal output with low sample and reagent volumes. From Figure 5, it can be observed that a 3-fold increase in the CAb concentration and 8-fold increase in the DAb concentration, relative to conventional concentrations, gives a 5-fold higher SNR. The much higher increase in DAb concentration is attributed to the smaller molecular size of the rat TNF-α DAb, requiring a greater demand for binding on the chamber surface. Thus, the sandwich ELISA protocol was successfully optimized using the Optimiser microfluidic microplate to obtain maximum sensitivity on the developed LOC. Rat TNF-α concentrations ranging from 62.5 to 4000 pg/mL were detected using optimal CAb (16.0 μg/mL) and DAb (4.0 μg/mL) concentrations with the Optimiser microfluidic microplate. Assay results are shown in Figure 6. The enumerated results had a trend similar to that

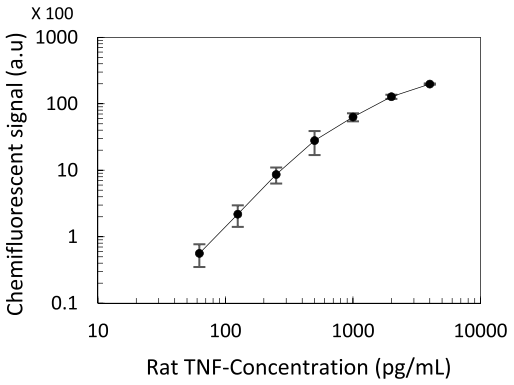

Figure 6. Standard curve obtained from an Optimiser microfluidic microplate based CF assay for detecting rat TNF-α with optimized antibody concentration. Each point represents the mean of three replicates.

of conventional 96-well plate results shown in Figure 4, which validated the assay results from Optimiser microfluidic microplate.

RESULTS AND DISCUSSION

Preparation of LOC for Assay. The developed LOC has a very low surface energy due to the inherent hydrophobic nature of COC. In order to prevent nonspecific binding of proteins in the reagent reservoirs of the LOC, the detection antibody chamber and sample loading chamber were made hydrophilic using a biocompatible hydrophilic coatings for COC, P100d (Joninn, Denmark), and dried before immunoassay reagents were loaded for long-term storage before performing the POC assay. The following preparation steps are required for the LOC assay. First, 16.0 μg/mL of TNF-α CAb and 5.0 μg/mL of Goat Anti-Mouse IgG were coated in the test and positive control spiral reaction chambers, respectively. All three spirals were then blocked, making that with no antibody the negative control. In the next step, 25.0 μL of the HRP-conjugated detection antibody was loaded onto the DAb chamber. SuperSignal ELISA Pico CL Substrate was loaded into the washing buffer chamber and substrate chamber, respectively.

Performance of Enzyme Immunoassay on LOC for Point of Care Testing (POCT). After the preassay steps described above, typically LOC can be sealed with moisture-impermeable tape, packaged in an aluminum-coated pouch, and refrigerated at 4.0 °C until use with a real sample. Shelf life experiments are under evaluation to confirm the usability of the LOC as a true POCT device. Artificial serum (Serasub) samples with spiked rat TNF-α covering a range of target concentrations were loaded in the sample chamber of different LOCs, and air pressure was applied by an external pump with a flow rate of approximately 0.6−2.0 mL/min. Sequential delivery of the reagents was performed after each incubation step. Similar to the assay protocol followed in an Optimiser microfluidic microplate, after sample loading, external air pressure was applied through the air inlet until sample flowed through the test and control spiral reaction microchannels, followed by which the sample was incubated for 20 min. In the next step, HRP-conjugated Dab was pushed and incubated for 20 min, followed by which wash buffer was flowed through the spiral microchannels. In the last step, CL substrate was pressurized through the spiral microchannels and was allowed to incubate for 5 min. The CL signal output exhibited from the reaction between the CL substrate and HRP was observed to steeply increase for 5 min and was then saturated after 5 min. Hence, only after 5 min of CL substrate incubation was a stable and reliable CL signal output obtained. Finally, the CL signal outputs from the spiral reaction microchannels were acquired using a Synergy H1 (BioTek, USA) reader. The chemiluminescence signal from the test chamber is directly proportional to the concentration of rat TNF-α target in the sample. The positive control confirms the functional stability of the detection antibody and the substrate which renders the result relevant, while signals from the negative control chambers indicated the amount of nonspecific binding (background noise) for each LOC assay, respectively. Hence, this chip can be used in the field to obtain clinically relevant data on the spot. The entire sandwich assay process took less than 30 min to complete, which is a substantial reduction in time relative to the conventional assay time of 3−8 h. A schematic diagram of the analyzer system, with control functions of the air-driven flow and optical detection, is presented in Scheme 5. However, since a fully functional analyzer system is currently under development, the LOC was air-driven using a hybrid peristaltic microfluidic pump (Model EW-73160-31, Cole Palmer, USA) to perform the currently explained assay.

Evaluation of LOC Performance. The optimized capture and detection antibody concentrations obtained from previous

DOI: 10.1021/acs.analchem.9b00582
Anal. Chem. 2019, 91, 6652−6660

Scheme 5. Schematic Diagram of the Analyzer System with Control Functions of the Air-Driven Flow and Optical Detection[18]

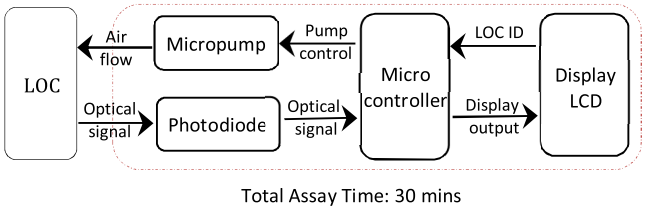

experiments were used for the CL detection of TNF-α in buffer solutions and plasma samples from RCS-exposed rats. As discussed, the number of CAb molecules immobilized on the surface of the spiral reaction channel of the LOC is much higher relative to the amount bound to each well of the 96-well plate because spirals have a 50 times higher surface to volume ratio; hence, a large number of antigen binding sites are available. Therefore, even a very low concentration of TNF-α antigen in the sample can specifically bind to the CAbs. The CL response of the LOC for different TNF-α target concentrations for POCT use is presented in Figure 7. A

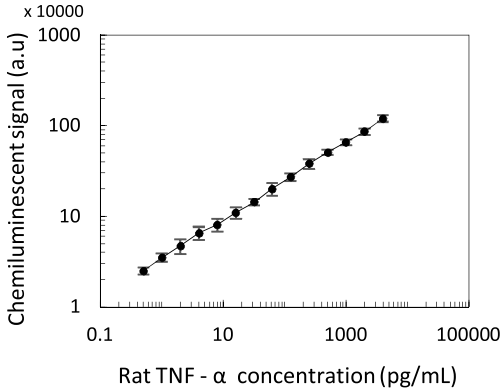

Figure 7. Chemiluminescent signal output for different target concentrations performed in the LOC for point of care detection of TNF-α. Each point represents the mean of three replicates.

linear trend was observed over a wide concentration range, from 0.5 pg/mL to 4.0 ng/mL. The LOC device successfully detected low amounts of antigen in a clinically relevant range which were in concurrence with results from studies related to the detection of pneumoconiosis in coal workers.[33] Thus, the LOC could be used as a POC screening test for detection of early effects of RCS exposure and the prevention of disease progression. The limit of detection (LOD) for the LOC device was calculated as LOD = limit of blank (LOB) + 3 × (SD for lowest concentration sample with a CF signal higher than blank), and the LOB was calculated as LOB = mean blank response + 3 × (SD blank), where SD is the standard deviation. All analyte concentrations were analyzed in triplicate. On the basis of the CL signal output shown in Figure 7, target protein recovery in artificial serum was observed to be 94%, which falls within the acceptable recovery range. Assay performance using the LOCs achieved a wider dynamic range and 20 times lower LOD (0.5 pg/mL) relative to the conventional 96-well plate assay. The average CV and interassay variability calculated from three replicates at each concentration ranged from about 5% to 8%, with an overall linear trend.

Evaluation of TNF-α in Plasma of Rats Exposed to RCS. *Rat Samples Exposed to RCS.* RCS exposure of rats to induce pulmonary toxicity was conducted in a laboratory for animal care (NIOSH, Morgantown, WV) following an animal protocol approved by the institutional Animal Care and Use Committee (ACUC). The inhalation exposure protocol has been described in our previous publication.[34] Briefly, pathogen-free male Fisher rats (Charles River Laboratories, Wilmington, MA) weighing approximately 150 g were allowed to acclimatize for about 10 days following their arrival to the Animal Facility. The rats were housed in ventilated cages under environmentally controlled conditions and were provided food and tap water.

Groups of rats were exposed to filtered air (control) and crystalline silica (Min-U-Sil silica, US Silica, Berkley Springs, WV) by inhalation (15.0 mg/m^3, 6 h/day, for five consecutive days).The exposure conditions (concentration of silica and duration of inhalation exposure) were selected on the basis of the results of studies reported from our laboratory.[34] Exposure of rats to RCS under the selected conditions are known to result in pulmonary response following various latency periods.[34]

Following termination of exposure to air or silica aerosol, the control and silica-exposed rats were maintained for up to 1 year on a 12 h light−dark schedule with free access to food and tap water. At postsilica exposure time intervals of 1 and 12 months, the control and silica-exposed rats were euthanized, and blood was drawn into vacutainer tubes containing EDTA as anticoagulant. The blood samples were centrifuged at 2000 rpm for 10 min to separate plasma from the blood cells. The plasma samples were kept frozen at −80 °C until used. When they were used, the samples were thawed quickly by placing the vials in a water bath maintained at 37 °C. Any short-term storage was at −20 °C in a refrigerator. For further validation of the functionality of the fabricated LOC, plasma samples from respirable silica-exposed rats were tested using the developed LOCs. The rat plasma was obtained from the NIOSH/Health Effects Laboratory Division (HELD, Morgantown, WV). Plasma samples from rats were collected 1 month and 1 year after exposure (6 h/day, for 5 consecutive days) and tested for TNF-α. The CL responses to plasma samples from the unexposed (i.e., controls exposed to air) and RCS-exposed groups are shown in Figure 8. The CL output signal of the LOC assay for unexposed rats was close to the background signal of the LOC ELISA, but the CL responses for the RCS-exposed rats were elevated, from around 16.0 to 32.0 pg/mL and from 1.0 to 2.0 ng/mL, for postexposure periods of 1 month and 1 year, respectively. These results indicated that RCS exposure results in pulmonary toxicity in rats, as evidenced by elevated TNF-α concentrations, at both postexposure time intervals. Additionally, the pulmonary response is progressive, continuing even after silica exposure stops. This result was consistent with those from previous studies on gene expression profiling and on the time course of pulmonary response of rats to inhalation of crystalline silica.[20,35] Therefore, on the basis of results from both spiked samples and RCS-exposed rats, the developed LOC has the potential for detecting an inflammatory response to RCS at an early stage, before pulmonary health effects associated with exposure become severe. Also, because the LOC platform employs ELISA methods that are widely used for laboratory

DOI: 10.1021/acs.analchem.9b00582
Anal. Chem. 2019, 91, 6652−6660

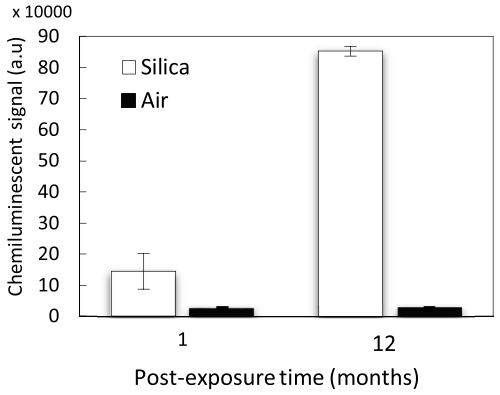

Figure 8. CL signal output for detection of TNF-α in plasma samples obtained from rats exposed to silica for 1 month and 1 year. The control signal was obtained from plasma samples of rats exposed to nontoxic air for 1 month and 1 year, respectively.

measurement of a wide range of biomarkers, the developed LOC has the potential for measurement of many other biomarkers of interest useful for exposure assessment and health surveillance. The developed LOC uses a very low sample volume of 20 μL and provides quantitative results within 30 min. The COC chips are mass-fabricated using high-throughput injection molding, and volumes of immunoassay reagents used in LOC are much lower than those used in conventional 96-well plate techniques. Hence, the developed LOC is cost effective and acts as an ideal POCT platform with rapid diagnostics time in comparison to the high-cost and labor-intensive 96-well plate methods.

CONCLUSION

The development of microfluidic devices for POCT applications is a field of constant growth, but their fabrication can require expensive clean-room facilities and materials. On the opposite end of the spectrum, paper or strip-based devices are inexpensive but have limited applicability, sensitivity, and accuracy. For the first time, we have demonstrated a complete process of ELISA development and optimization using a robust, polymer-based LOC for detecting TNF-α, an important biomarker with the potential for disease prevention in millions of workers globally. The low LOD of the developed LOC makes it possible to detect biological response to RCS exposure at a very early stage with point of care convenience. The simplified, cost-effective LOC test eliminates the need for expensive, time-consuming analyzes in off-site laboratories, thereby making it useful for routine, on-site health screenings. For implementation of a complete POCT diagnostic system, an inexpensive portable analyzer compatible with the developed LOC is required for accurate, quantitative results. Development of a hand-held analyzer that can be interfaced with the developed LOC for field applications is underway. The injection-molded COC chip, reported in this work, can perform highly sensitive CL-based ELISA assays using preloaded reagents that flow sequentially through a sensing chamber. Thus, the developed LOC device represents a major step toward development of an autonomous, sample to answer POCT platform that is user friendly, robust, and cost effective.

AUTHOR INFORMATION

Corresponding Authors

*E-mail for B.K.K.: bku@cdc.gov.

*E-mail for C.H.A.: ahnch@ucmail.uc.edu.

ORCID

V. Thiyagarajan Upaassana: 0000-0003-0468-596X

Author Contributions

All authors have given approval to the final version of the manuscript.

Notes

The authors declare no competing financial interest.

ACKNOWLEDGMENTS

We are very grateful for the funding provided by NIOSH-CDC (Contract No.: 212-2015-M-62326 and #75D3-0118-C-00391) under the NORA projects 939039G and 93908LQ for student and research materials support. The authors would like to thank Dr. Kevin Asley and Dr. Amos Doepke for their helpful comments on this work. We also thank Dr. Jerry Smith at NIOSH/DART for helpful comments on immunoassay test agents, Dr. Dale Porter at NIOSH/HELD for helpful comments on biomarkers of silica exposure and its effect, Pramod Kulkarni at NIOSH/DART for suggestions on the study, John Snawder at NIOSH/DART for assistance, and Dr. Gayle DeBord at NIOSH/DART for strong support on the project.

REFERENCES

(1) Occupational Safety and Health Administration, US Department of Labor, 2013, proposed rule [Docket No. OSHA-2010-0034]. http://www.gpo.gov/fdsys/pkg/FR-2013-09-12/pdf/2013-20997.pdf.

(2) National Institute for Occupational Safety and Health. NIOSH hazard review. Health effects of occupational exposure to respirable crystalline silica. Washington, DC, US Department of Health and Human Services, CDC, National Institute for Occupational Safety and Health, 2002; DHHS (NIOSH) publication no. 2002-129. http://www.cdc.gov/niosh/docs/2002-129/pdfs/2002-129.pdf.

(3) OSHA NIOSH Hazard Alert, 2012. https://www.osha.gov/dts/hazardalerts/hydraulic_frac_hazard_alert.pdf.

(4) Occupational Exposure Limit Evaluation: Silica, Crystalline Quartz, 2014. https://pdfs.semanticscholar.org/b62b/7d730fc2ef8deec827e.b82e8ce7db49e9a2b.pdf.

(5) Esswein, E. J.; Breitenstein, M.; Snawder, J.; Kiefer, M.; Sieber, W. K. *J. Occup. Environ. Hyg.* **2013**, *10*, 347−356.

(6) BLS, 2014, *Quarterly Census of Employment and Wages*. http://www.bls.gov/cew/.

(7) Occupational Safety and Health Administration, US Department of Labor, 2016, final rule. (Docket No. OSHA-2010-0034). http://www.gpo.gov/fdsys/pkg/FR-2013-09-12/pdf/2013-20997.pdf.

(8) Chisholm, J. *Indoor Built Environ.* **1999**, *8*, 94−106.

(9) Gulumian, M.; Borm, P. J.; Vallyathan, V.; Castranova, V.; Donaldson, K.; Nelson, G.; Murray, J. *J. Toxicol. Environ. Health, Part B* **2006**, *9*, 357−395.

(10) Qiu, Z.; Shu, J.; Tang, D. *Anal. Chem.* **2017**, *89*, 5152−5160.

(11) Ren, R.; Cai, G.; Yu, Z.; Zeng, Y.; Tang, D. *Anal. Chem.* **2018**, *90*, 11099−11105.

(12) Luo, Z.; Zhang, L.; Zeng, R.; Su, L.; Tang, D. *Anal. Chem.* **2018**, *90*, 9568−9575.

(13) Xianyu, Y.; Zhu, K.; Chen, W.; Wang, X.; Zhao, H.; Sun, J.; Wang, Z.; Jiang, X. *Anal. Chem.* **2013**, *85*, 7029−7032.

(14) Chen, Y.; Xianyu, Y.; Wu, J.; Dong, M.; Zheng, W.; Sun, J.; Jiang, X. *Anal. Chem.* **2017**, *89*, 5422−5427.

(15) Sharma, S.; Zapatero-Rodríguez, J.; Estrela, P.; O'Kennedy, R. *Biosensors* **2015**, *5*, 577−601.

(16) Peeling, R. W.; Mabey, D. *Clin. Microbiol. Infect.* **2010**, *16*, 1062−1069.

(17) Foudeh, A. M.; Didar, T. F.; Veres, T.; Tabrizian, M. *Lab Chip* **2012**, *12*, 3249−66.

DOI: 10.1021/acs.analchem.9b00582
Anal. Chem. 2019, 91, 6652−6660

(18) Jung, W.; Han, J.; Kai, J.; Lim, J. Y.; Sul, D.; Ahn, C. H. *Lab Chip* **2013**, *13*, 4653−62.
(19) Tiwari, R. R. *Indian Journal of Occupational and Environmental Medicine* **2005**, *9*, 103.
(20) Porter, D. W.; Ye, J.; Ma, J.; Barger, M.; Robinson, V. A.; Ramsey, D.; McLaurin, J.; Khan, A.; Landsittel, D.; Teass, A.; Castranova, V. *Inhalation Toxicol.* **2002**, *14*, 349−367.
(21) Morfeld, P.; Borm, P. A.; Schins, R. F.; Lenaerts, H.; Witte, B.; Derwall, R.; Piekarski, C. *Biomarkers* **2001**, *6*, 428−39.
(22) Huaux, F. *Current opinion in allergy and clinical immunology* **2007**, *7*, 168−73.
(23) Pandey, J. K.; Agarwal, D. *Indian journal of occupational and environmental medicine* **2012**, *16*, 101.
(24) Slavov, E.; Miteva, L.; Prakova, G.; Gidikova, P.; Stanilova, S. *Toxicol. Ind. Health* **2010**, *26*, 479−86.
(25) Piruska, A.; Nikcevic, I.; Lee, S. H.; Ahn, C. H.; Heineman, W. R.; Limbach, P. A.; Seliskar, C. J. *Lab Chip* **2005**, *5*, 1348−54.
(26) Ahn, C. H.; Choi, J. W.; Beaucage, G.; Nevin, J. H.; Lee, J. B.; Puntambekar, A.; Lee, J. Y. *Proc. IEEE* **2004**, *92*, 154−173.
(27) Kai, J.; Puntambekar, A.; Santiago, N.; Lee, S. H.; Sehy, D. W.; Moore, V.; Han, J.; Ahn, C. H. *Lab Chip* **2012**, *12*, 4257−4262.
(28) https://resources.rndsystems.com/pdfs/datasheets/dy510.pdf.
(29) Cinquanta, L.; Fontana, D. E.; Bizzaro, N. *Autoimmunity Highlights* **2017**, *8*, 9.
(30) Assay Transfer Guide: For transfer of validated 96-well ELISA to Optimiser, Mico BioMed USA Inc., Inc. 2011. Available at http://siloambio.com/wp-content/uploads/2012/12/opti-2-ms-0053-a0_assay-transfer-guide-1.pdf.
(31) Thermo Scientific Pierce Assay Development Technical Handbook, Thermo Scientific, 2011. Available at https://tools.thermofisher.com/content/sfs/brochures/1602127-Assay-Development-Handbook.pdf.
(32) Rey, E. G.; O'Dell, D.; Mehta, S.; Erickson, D. *Anal. Chem.* **2017**, *89*, 5095−5100.
(33) Lee, J. S.; Shin, J. H.; Lee, J. O.; Lee, K. M.; Kim, J. H.; Choi, B. S. *SH W* **2010**, *1*, 69−79.
(34) Sellamuthu, R.; Umbright, C.; Roberts, J. R.; Chapman, R.; Young, S. H.; Richardson, D.; Leonard, H.; McKinney, W.; Chen, B.; Frazer, D.; Li, S. *Toxicol. Sci.* **2011**, *122*, 253−264.
(35) Porter, D. W.; Hubbs, A. F.; Mercer, R.; Robinson, V. A.; Ramsey, D.; McLaurin, J.; Khan, A.; Battelli, L.; Brumbaugh, K.; Teass, A.; Castranova, V. *Toxicol. Sci.* **2004**, *79*, 370−380.

DOI: 10.1021/acs.analchem.9b00582
Anal. Chem. 2019, 91, 6652−6660